Theoretical description of spherically confined, strongly correlated Yukawa plasmas

H. Bruhn, H. Kählert, T. Ott, and M. Bonitz[*]

Institut für Theoretische Physik und Astrophysik, Christian-Albrechts-Universität zu Kiel, D-24098 Kiel, Germany

J. Wrighton and J. W. Dufty

Department of Physics, University of Florida, Gainesville, Florida 32611, USA

A theoretical description of the radial density profile for charged particles with Yukawa interaction in a harmonic trap is described. At strong Coulomb coupling shell structure is observed in both computer simulations and experiments. Correlations responsible for such shell structure are described here using a recently developed model based in density functional theory. A wide range of particle number, Coulomb coupling, and screening lengths is considered within the fluid phase. A hypernetted chain approximation shows the formation of shell structure, but fails to give quantitative agreement with Monte Carlo simulation results at strong coupling. Significantly better agreement is obtained within the hypernetted chain structure using a renormalized coupling constant, representing bridge function corrections.

PACS number(s): 52.27.Gr, 52.27.Lw, 52.65.Yy

I. INTRODUCTION

Spatially confined charged particles have attracted growing interest. Examples include electrons in quantum dots [1], ions in Penning and Paul traps [2,3], and the mesoscopic charges of dusty plasmas [4,5]. In particular, three-dimensional classical spherical plasmas have been produced in ion systems [6] and more recently in dusty plasmas [7]. The structural and dynamic properties of these systems continue to attract the interest of many groups in various fields; e.g., [8–10].

At sufficiently strong coupling these systems form concentric shells which are well reproduced by simulations; see [11–13] and references therein. The objective here is to provide a theoretical analysis to complement these results from simulation and experiments, for a better physical understanding of the underlying mechanisms. For harmonically confined particles with Coulomb interaction such a theory of shell formation as a function of temperature (inverse coupling) was derived recently using classical density functional theory (DFT) [14–16]. However, a special property of dusty plasmas is the screening of the pair interaction. The theoretical description is extended here to describe spherically trapped strongly correlated particles with Yukawa interaction for such dusty plasmas.

The state conditions are specified by three dimensionless parameters: particle number N, coupling constant Γ (defined below), and dimensionless screening parameter κ^*. The ranges of values considered are $15 < N < 500$, $0 < \Gamma < 100$, and $0 < \kappa^* \leqslant 1$. The primary focus here is on shell formation as a function of these parameters. Only the equilibrium fluid phase is considered (rotational invariance) so that shell structure is reflected in the radial dependence of the density of confined charges. The average density is defined as a multidimensional configuration integral in the canonical ensemble, which can be evaluated by Monte Carlo simulation. New simulations are provided here as a means to determine the accuracy of theoretical approximations. The system, dimensionless

units, and adaptation of the hypernetted chain (HNC) theory introduced in [15] for confined Coulomb charges are described in Sec. II A. The density profiles from the HNC approximation are compared to simulations in Sec. III. It is found that the formation of shells, as well as their location and populations, is well described by the HNC approximation, but the shell maxima and widths show large discrepancies for $\Gamma > 10$ and the errors increase with increasing κ^*. The primary qualitative effect of screening is to shift the shells toward the center and decrease the overall volume. An "adjusted" hypernetted chain approximation (AHNC) is considered in Sec. IV. This is based on a model for the bridge function corrections to HNC first introduced by Ng [17] for the pair distribution function of a Coulomb one-component plasma (OCP). It has the property of preserving the form of the HNC equations with only a renormalization of Γ to some larger effective value. It is shown that the same method applies to the Yukawa OCP for accurate pair correlations even at very strong coupling, and the approach is then applied to the bridge corrections to the equation for the density profile. An optimized renormalization for the density leads to excellent results for the Coulomb case (e.g., $\Gamma \leqslant 100, N \leqslant 500$). For Yukawa systems this approach is very useful as well for the radial distribution function, but it is somewhat more limited for the density profile at larger values of κ^* and N.

II. THEORY AND SIMULATION

A. Model and units

The system is comprised of N identical charges interacting pairwise via a Yukawa potential, confined by a harmonic potential centered at the origin. The Hamiltonian is

$$H = \sum_{i=1}^{N} \left(\frac{1}{2} m v_i^2 + \frac{1}{2} m \omega^2 r_i^2 \right) + \frac{1}{2} \sum_{i \neq j=1}^{N} V(r_{ij}). \quad (1)$$

[*]bonitz@physik.uni-kiel.de

Here m is the mass, ω is the angular frequency measuring the strength of the confinement, and $\mathbf{r}_i, \mathbf{v}_i$ are the position and velocity of charge i. The Yukawa interaction is

$$V(r_{ij}) = q^2 \frac{e^{-\kappa r_{ij}}}{r_{ij}}, \qquad (2)$$

where $r_{ij} \equiv |\mathbf{r}_i - \mathbf{r}_j|$, q is the particle charge, and κ is an inverse screening length. The physical origin of this screening length is described elsewhere [5] and will not be discussed here. The primary property of interest here is the local density of charges in the trap at equilibrium. For the classical canonical ensemble its dimensionless form is given by

$$n^*(r_1^*) \equiv n(r_1) r_0^3 = N \frac{\int d\mathbf{r}_2^* \dots d\mathbf{r}_N^* e^{-V^*(\mathbf{r}_1^*, \dots, \mathbf{r}_N^*)}}{\int d\mathbf{r}_1^* \dots d\mathbf{r}_N^* e^{-V^*(\mathbf{r}_1^*, \dots, \mathbf{r}_N^*)}}, \qquad (3)$$

with

$$\begin{aligned} V^*(\mathbf{r}_1^*, \dots, \mathbf{r}_N^*) &\equiv \beta V(\mathbf{r}_1, \dots, \mathbf{r}_N) \\ &= \Gamma \left[\frac{m\omega^2 r_0^3}{2q^2} \sum_{i=1}^{N} r_i^{*2} + \frac{1}{2} \sum_{i \neq j=1}^{N} \frac{e^{-\kappa^* r_{ij}^*}}{r_{ij}^*} \right]. \end{aligned} \qquad (4)$$

Here, $\mathbf{r}_i^* = \mathbf{r}_i / r_0$, $\beta = 1/k_B T$ is the inverse temperature, $\Gamma = \beta q^2 / r_0$ is the Coulomb coupling constant, and $\kappa^* = \kappa r_0$. The usual choice for the length scale r_0 is the ion sphere radius, or mean distance between charges, given by

$$4\pi r_0^3 \bar{n}/3 = 1, \qquad (5)$$

where $\bar{n}$ is a characteristic spatially averaged density to be chosen for convenience. Here it is chosen to simplify the Hamiltonian by the condition

$$\frac{m\omega^2 r_0^3}{2q^2} = \frac{1}{2}, \quad \text{or} \quad \bar{n} = \frac{3m\omega^2}{4\pi q^2}. \qquad (6)$$

This is not the average density for the Yukawa particles in the trap $\bar{n}_T = N/V_T$, where the volume $V_T = 4\pi R_T^3/3$ is defined by the maximum radius R_T at which the force on a charge due to the trap is equal to that of all other charges

$$m\omega^2 R_T = q^2 \int d\mathbf{r}' \frac{e^{-\kappa|\mathbf{R}_T - \mathbf{r}'|}}{|\mathbf{R}_T - \mathbf{r}'|^2} (1 + \kappa|\mathbf{R}_T - \mathbf{r}'|) n_T(r'). \qquad (7)$$

It follows that $\bar{n}_T = \bar{n}$ for $\kappa = 0$ and $\bar{n}_T > \bar{n}$ for $\kappa > 0$. The solution to (7) is discussed further below.

The dimensionless trap potential energy is now a function of two dimensionless parameters, the Coulomb coupling strength Γ and the screening parameter κ^*,

$$V^*(\mathbf{r}_1^*, \dots, \mathbf{r}_N^*) = \Gamma \frac{1}{2} \left[\sum_{i=1}^{N} r_i^{*2} + \sum_{i \neq j}^{N} \frac{e^{-\kappa^*|\mathbf{r}_i^* - \mathbf{r}_j^*|}}{|\mathbf{r}_i^* - \mathbf{r}_j^*|} \right], \qquad (8)$$

and the dimensionless density profile $n^*(r^*)$ can be obtained numerically from a Metropolis Monte Carlo simulation for given Γ, κ^*, and N.

B. Theory and approximations

A formal representation of the average density profile was developed within density functional theory in Ref. [15]. That analysis applies here as well, with only the replacement of the Coulomb potential by the Yukawa potential. First, the density

is represented in terms of a dimensionless effective potential $U^*(r^*)$,

$$n^*(r^*) \equiv \overline{N} \frac{e^{-\Gamma U^*(r^*)}}{4\pi \int_0^\infty dr^* r^{*2} e^{-\Gamma U^*(r^*)}}. \qquad (9)$$

Here $\overline{N}$ denotes the average number of particles in the trap, since the theory is formulated in the grand canonical ensemble. The effective potential obeys the equation

$$U^*(r^*) = \frac{1}{2} r^{*2} + \overline{N} \frac{\int d\mathbf{r}^{*\prime} e^{-\Gamma U^*(r^{*\prime})} \overline{c}(|\mathbf{r}^* - \mathbf{r}^{*\prime}|)}{\int d\mathbf{r}^{*\prime} e^{-\Gamma U^*(r^{*\prime})}} + B(r^*). \qquad (10)$$

The function $\overline{c}(r^*)$ is proportional to the direct correlation function for a uniform one-component plasma (OCP) of Yukawa charges

$$\overline{c}(r^*) = -\frac{1}{\Gamma} c_{OCP}(r^*), \qquad (11)$$

which is related to the OCP radial distribution function $g_{OCP}(r^*)$ by the Ornstein-Zernike equation

$$\begin{aligned} g_{OCP}(r^*) - 1 &= c_{OCP}(r^*) + \overline{n}_{OCP}^* \int d\mathbf{r}^{*\prime} [g_{OCP}(r^{*\prime}) - 1] \\ &\times c_{OCP}(|\mathbf{r}^* - \mathbf{r}^{*\prime}|). \end{aligned} \qquad (12)$$

Finally, $g_{OCP}(r^*)$ is determined from the equation

$$\begin{aligned} \ln g_{OCP}(r^*) &= -\Gamma \frac{e^{-\kappa^* r^*}}{r^*} + \overline{n}_{OCP}^* \int d\mathbf{r}^{*\prime} [g_{OCP}(r^{*\prime}) - 1] \\ &\times c_{OCP}(|\mathbf{r}^* - \mathbf{r}^{*\prime}|) - \Gamma B_{OCP}(r^*). \end{aligned} \qquad (13)$$

The second term of (10) describes the effect of correlations among particles in the trap in terms of the corresponding correlations among particles in the uniform OCP. The last term $B(r^*)$ corrects this approximate treatment of correlations and is known as a bridge function. Similarly, $B_{OCP}(r^*)$ is the bridge function for $g_{OCP}(r^*)$ [18]. To optimize this contribution of OCP correlations, the density of the trap is matched to that of the OCP:

$$\overline{n}_{OCP}^* = \overline{n}_T^*. \qquad (14)$$

For given $\overline{N}$ the trap density is fixed by the volume of the trap, whose radius R_T must be calculated from (7). An approximate evaluation for the ground state has been discussed elsewhere [19], with the result that it is the unique positive, real solution to

$$\begin{aligned} &-(1 + \kappa^* R^*)(\overline{N} - 1) + R^{*3} + \kappa^* R^{*4} \\ &+ \frac{6}{15} \kappa^{*2} R^{*5} + \frac{1}{15} \kappa^{*3} R^{*6} = 0. \end{aligned} \qquad (15)$$

In all of the following, $\overline{n}_T^*$ is determined in this way for each κ^*.

The above Eqs. (9)–(13) are still exact, but require specification of the bridge functions. The simplest approximation is the neglect of the bridge functions, leading to the hypernetted

chain approximation (HNC)

$$U_{\mathrm{HNC}}^*(r^*) = \frac{1}{2}r^{*2} + \overline{N}\frac{\int d\mathbf{r}^{*\prime}e^{-\Gamma U_{\mathrm{HNC}}^*(r^{*\prime})}\overline{c}_{\mathrm{HNC}}(|\mathbf{r}^* - \mathbf{r}^{*\prime}|)}{\int d\mathbf{r}^{*\prime}e^{-\Gamma U_{\mathrm{HNC}}^*(r^{*\prime})}},$$

(16)

$$\ln g_{\mathrm{HNC}}(r^*) = -\Gamma\frac{e^{-\kappa^* r^*}}{r^*} + \overline{n}_{\mathrm{T}}^*\int d\mathbf{r}^{*\prime}[g_{\mathrm{HNC}}(r^{*\prime}) - 1]$$
$$\times c_{\mathrm{HNC}}(|\mathbf{r}^* - \mathbf{r}^{*\prime}|),$$

(17)

$$g_{\mathrm{HNC}}(r^*) - 1 = c_{\mathrm{HNC}}(r^*) + \overline{n}_{\mathrm{T}}^*\int d\mathbf{r}^{*\prime}[g_{\mathrm{HNC}}(r^{*\prime}) - 1]$$
$$\times c_{\mathrm{HNC}}(|\mathbf{r}^* - \mathbf{r}^{*\prime}|).$$

(18)

This is a closed set of equations for $U_{\mathrm{HNC}}^*, g_{\mathrm{HNC}}(r^*)$, and $\overline{c}_{\mathrm{HNC}}$. Note that the determination of $g_{\mathrm{HNC}}(r^*)$ and $\overline{c}_{\mathrm{HNC}}$ is independent of the trap density calculation.

It is well known that the HNC approximation for the OCP properties is a good approximation except for strong coupling where the bridge function B_{OCP} becomes important. However, the results below for the trap density show that the trap bridge function can be important even at moderate coupling. It is therefore necessary to go beyond HNC and find an approximation for the bridge functions. This is described below.

III. RESULTS: HNC APPROXIMATION

Correlations in the HNC approximation are described by $\overline{c}_{\mathrm{HNC}}$. For weak coupling, $\Gamma < 1$, $\overline{c}_{\mathrm{HNC}} \to e^{-\kappa^* r^*}/r^*$. This is the "mean field" limit. Figure 1 shows a comparison of this mean field description with Monte Carlo simulation results at moderate coupling, $\Gamma = 1$ and 5 for several values of κ^*. As
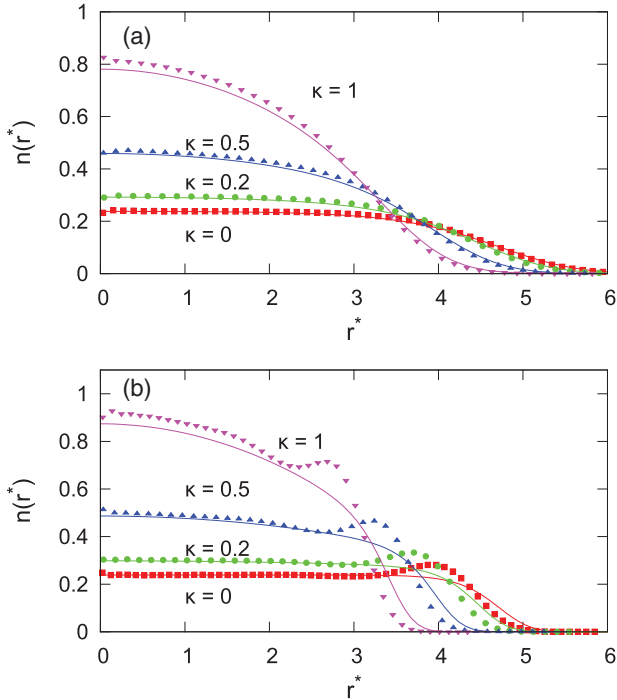

FIG. 1. (Color online) Mean field results for the density profile (lines) for a Coulomb and Yukawa OCP in a spherical trap for (a) $\Gamma = 1$ and (b) $\Gamma = 5$ for $N = 100$ compared with Monte Carlo simulations (symbols).
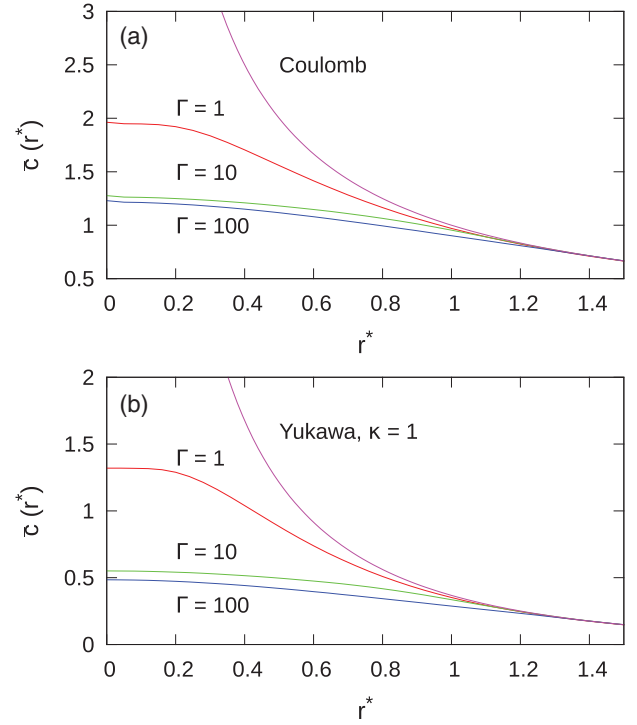

FIG. 2. (Color online) Various direct correlation functions for (a) Coulomb interaction and (b) Yukawa interaction with $\kappa^* = 1$. The top curve is the mean field value.

might be expected, there is reasonable agreement at $\Gamma = 1$, but emergence of an outer shell is evident at $\Gamma = 5$, which cannot be reproduced by the mean field theory. Evidently, here it is necessary to calculate the correlations of $\overline{c}_{\mathrm{HNC}}$ through the full coupled set of equations (16)–(18).

Figures 2(a) and 2(b) show $\overline{c}_{\mathrm{HNC}}$ as a function of r^* for $\kappa^* = 0$ and 1. In both cases the deviation from the mean field limit increases for stronger coupling, creating a "correlation hole" for $r^* < 1$. The effects of these correlations on the trap density profile are illustrated for several values of the screening parameter κ^* in Fig. 3 at $\Gamma = 50, N = 100$. It is seen that increased screening tends to compress the system [11] and enhance the shell structure.

The quality of HNC is tested by comparison to Monte Carlo simulations. This is illustrated for $N = 100$ and $\Gamma = 10, 40, 100$ with $\kappa^* = 0$ in Fig. 4(a) and with $\kappa^* = 1$ in Fig. 4(b). HNC is a poor approximation at $r^* = 0$ which results
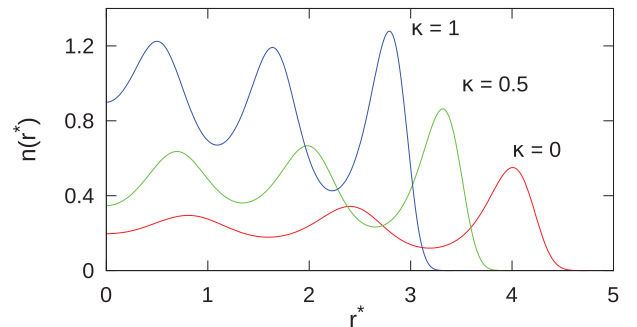

FIG. 3. (Color online) HNC density profile for a Yukawa system with various κ^* at $\Gamma = 50$ and $N = 100$.
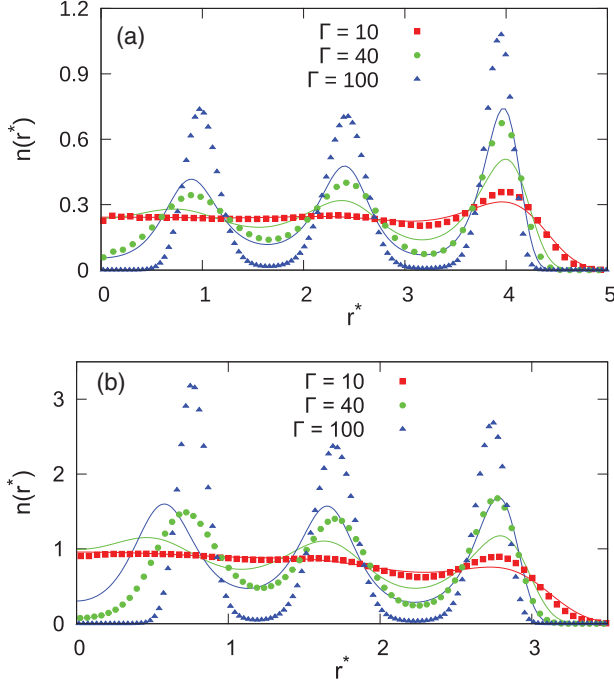
FIG. 4. (Color online) Density profile for $N = 100$ particles and various Γ values: comparison of HNC results (solid lines) with Monte Carlo (symbols) for (a) Coulomb and (b) Yukawa interaction with $\kappa^* = 1$.
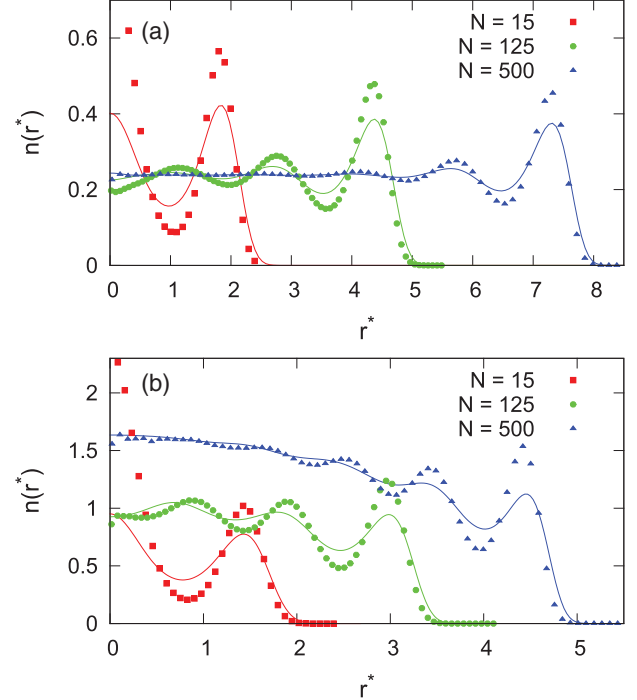

FIG. 5. (Color online) Density profile for $\Gamma = 20$: comparison of HNC results (lines) with Monte Carlo results (symbols) for (a) Coulomb and (b) Yukawa interaction with $\kappa^* = 1$.

in overall poor results for small particle numbers $\overline{N} < 10$. This error appears periodically with the creation of each new shell and is small if no particle is at the center. For $\kappa^* = 0$ the shell locations match well the simulation data, while increasing κ^* leads to decreased accuracy for the inner shells. The effect is small up to $\kappa^* = 0.5$. Figure 5 compares HNC and Monte Carlo results with $N = 15$, 125, and 500 for Coulomb charges in Fig. 5(a), and for Yukawa charges with $\kappa^* = 1$ in Fig. 5(b). The shell populations (not shown) and locations are nearly independent of Γ, as seen in MC simulations [20,21], and are given accurately by HNC. However, the peak heights and widths for the shells are poorly predicted and require going beyond the HNC approximation.

IV. ADJUSTED HNC

In a recent analysis for Coulomb systems in a spherical trap it was also observed that the HNC approximation gives the correct location and population of shells [14,16], which depend only weakly on Γ. For Yukawa systems, these properties become less accurate with increasing κ^*. For both Coulomb and Yukawa, the amplitude and width depend strongly on Γ and are underestimated by the HNC approximation at strong coupling. This suggests that increasing the coupling constant alone would increase the accuracy of HNC.

A. Pair distribution function

This failure of HNC for strong coupling has been studied in some detail for the calculation of the Coulomb $g_{OCP}(r)$. Among the earliest investigations is that of Ng [17] who observed that the HNC peak positions are given accurately for strong

coupling, but not the amplitudes and widths. He corrected the HNC by representing the bridge function of (13) in the form

$$B_{OCP}(r^*) \to \lambda(\Gamma)\beta V(r^*),\qquad(19)$$

where $\lambda(\Gamma)$ is a chosen function of Γ and $V(r^*)$ is the Coulomb potential. This particular choice was not obtained from any theoretical analysis, but rather because it leads back to the HNC form with a renormalized coupling constant $\Gamma' = [1 + \lambda(\Gamma)]\Gamma$. This approach will be referred to as the adjusted HNC (AHNC). It was shown that an accurate prediction of $g_{OCP}(r)$ could be obtained over the entire fluid domain with the choice

$$\lambda(\Gamma) \to \lambda_{Ng}(\Gamma) = 0.6 \, erf(0.024\Gamma).\qquad(20)$$

Subsequent theoretical studies of the Coulomb bridge function by Rosenfeld and Ashcroft [22] indicated that it has a "universal" form and hence could be represented by the corresponding hard sphere bridge function for which an accurate parametrization is known. Although considerably more complex to implement computationally, it also gives a very good representation for $g_{OCP}(r)$. Furthermore, it has an important thermodynamic consistency not shared by the HNC or AHNC approximations. Evidently, the functional form (19) represents the actual bridge function for the relevant range of r needed to determine $g_{OCP}(r^*)$ (the numerical difficulty of determining $B_{OCP}(\mathbf{r}^*)$ precisely from $g_{OCP}(r^*)$ is discussed by Poll *et al*. [23]). Due to its simplicity and the direct interpretation as a renormalization of the coupling strength the AHNC will be used here as the means to improve the HNC approximation.

It remains to show how the bridge function should be chosen for the Yukawa potential. An empirical choice has been suggested in the form [24]

$$B_{\text{Y}}(\mathbf{r}^*) \rightarrow B_{\text{OCP}}(\mathbf{r}^*)e^{-\kappa^{*2}/2}, \qquad (21)$$

where $B_{\text{OCP}}(\mathbf{r}^*)$ is the Coulomb bridge function. This gives very good results for $g_{\text{Y}}(r^*)$ when $B_{\text{OCP}}(\mathbf{r}^*)$ is approximated by the corresponding hard sphere bridge function, as suggested by Rosenfeld and Ashcroft. In contrast the AHNC for the Yukawa potential is obtained from (19)

$$B_{\text{Y}}(\mathbf{r}^*) \rightarrow \lambda(\Gamma)\beta\frac{e^{-\kappa r}}{r}, \qquad (22)$$

where $\lambda(\Gamma)$ is the same form as (20) for the OCP

$$\lambda(\Gamma) \rightarrow \lambda_{\text{Ng}}(c(\kappa^*)\Gamma) = 0.6\,\text{erf}(c(\kappa^*)\Gamma). \qquad (23)$$

The constant $c(\kappa^*)$ is adjusted for each κ^*, with the Ng value $c(0) = 0.024$. This Yukawa AHNC leads to the HNC form (17), but with a renormalized coupling constant

$$\ln g_{\text{AHNC}}(r^*) = -\Gamma'\frac{e^{-\kappa^* r^*}}{r^*} + \bar{n}_{\text{T}}^* \int d\mathbf{r}^{*\prime}[g_{\text{AHNC}}(r^{*\prime}) - 1]$$
$$\times c_{\text{AHNC}}(|\mathbf{r}^* - \mathbf{r}^{*\prime}|). \qquad (24)$$

Figures 6(a) and 6(b) show the excellent agreement between AHNC and molecular dynamics even at very strong coupling for both $\kappa^* = 0$ and $\kappa^* = 2$. [Note that Γ and κ^* used here refer to a length unit r_0 defined by Eq. (5) with the OCP density.] It is interesting to note that results for recent MD simulations for different values of Γ and κ^* can be collapsed in terms of a single effective coupling constant $\Gamma^* = \Gamma^*(\Gamma, \kappa^*)$ [25]. In

summary the AHNC for $g(r^*)$ proposed by Ng for the Coulomb OCP works as well for the strongly coupled Yukawa plasma.

B. Density profile

With the results for the homogeneous OCP pair distribution function as a guide, a similar representation is considered for the bridge function $B(r|n)$ of the trap density profile (10):

$$B(r) \rightarrow \lambda(\Gamma)\beta V_0(r^*). \qquad (25)$$

Here βV_0 is the trap potential $\Gamma r^{*2}/2$, restoring the HNC form (9) and (16) with a renormalized Γ'. An initial approach would be to use the same renormalization function $\lambda(\Gamma)$ as obtained in the optimization of g_{AHNC}. This improves the accuracy for coupling constants up to $\Gamma \simeq 40$. To include stronger coupling it is necessary to choose a different renormalization function $\lambda(\Gamma)$ when calculating the trap density profile. Although Eqs. (19) and (25) formally allow for separate specifications of the renormalization function $\lambda(\Gamma)$ for the OCP and trap systems, results show that the same function $\lambda(\Gamma)$ must be used to determine the trap density profile to agree with simulations. That is, $\lambda(\Gamma)$ can be determined by fitting either the density profile or the pair correlation function, but not both.

The explanation as to why these two approaches [determining $\lambda(\Gamma)$ separately for the systems and as a common function] give very different results when using (19) and (25) lies in the relationship between direct correlation functions at different Γ. The scaled direct correlation function (11) is independent of Γ for $\Gamma > 10$. That is, if separate coupling constants for the trap (Γ_{trap}) and OCP (Γ_{OCP}) systems were fitted, the direct correlation functions are still related by

$$\frac{c(r; \Gamma_{\text{trap}})}{\Gamma_{\text{trap}}} = \frac{c(r; \Gamma_{\text{OCP}})}{\Gamma_{\text{OCP}}}. \qquad (26)$$

By considering again (10), this shows that the two procedures of using one common coupling constant, and using separate coupling constants, are related by scaling the number of particles in the trap. As the procedure of using a common renormalization function has shown to give good results, an equivalent approach involving separate renormalization functions is to have the effective number of particles in the trap also be dependent on the coupling constant so as to correct the discrepancy. It is important to note that with this alternative approach, although both the coupling constant and particle number are scaled, there still is only one fitting parameter for the trap (which fixes both a scaled coupling constant and particle number), and one fitting parameter for the OCP. However, the interpretation of the scaled particle number for the trap is not clear, as the shell structure depends critically on N.

Therefore we proceed by choosing to fit only the trap density profile, and using a common renormalization function for both the trap and the OCP systems.

An appropriate value of $\lambda(\Gamma)$ to optimize the density profile is obtained by minimizing the square difference of the Monte Carlo data $n_{\text{MC}}(r)$ and the HNC profile $n_{\text{HNC}}(r|\Gamma')$ with respect to Γ',
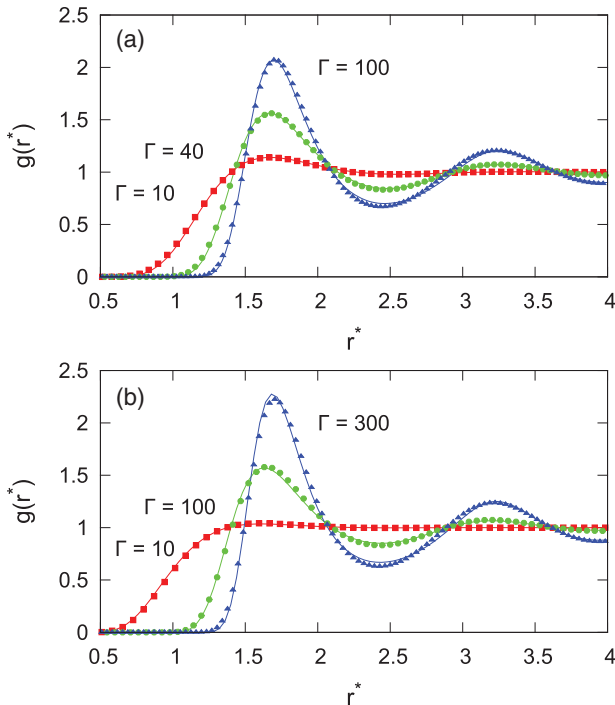

FIG. 6. (Color online) Comparison of AHNC results for the pair distribution function $g(r^*)$ with simulations for (a) Coulomb and (b) $\kappa^* = 2$. The values of Γ' in (a) are 12.5, 57, and 160; in (b) 10, 130, and 480.

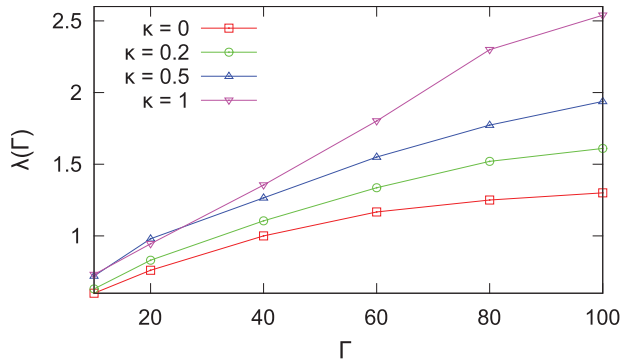$$\Gamma' : \min \int dr\, r^2 [n_{\text{MC}}(r|\Gamma) - n_{\text{HNC}}(r|\Gamma')]^2. \qquad (27)$$

FIG. 7. (Color online) Dependence of the AHNC parameter λ on Γ and κ^* calculated by (27) at fixed particle number $N = 100$. The renormalized coupling parameter is given by $\Gamma' = [1 + \lambda(\Gamma)]\Gamma$.

Since at small r the HNC density profile is not accurate, the difference in the peaks is weighted to the particle number in each shell. In practice this effectively fits the height and width of the outermost peak. The dependence of $\lambda(\Gamma, N)$ on Γ and N is shown in Figs. 7 and 8. The Γ dependence for different κ^* cannot be collapsed to a single curve by rescaling Γ as in Eq. (23), as the asymptotic large κ^* limits of $\lambda(\Gamma, N)$ are now different.

The quality of the AHNC approximation is again established by comparison to Monte Carlo data; see Fig. 9. AHNC describes accurately the density profile of Coulomb charges for the full range of Γ [Fig. 9(a)] and particle numbers N [Fig. 10(a)], while keeping the simple form of HNC. A similar improvement in accuracy is observed for the Yukawa system with $\kappa^* \leqslant 0.5$ and $N \leqslant 100$ [Fig. 9(b)]. For larger κ^* errors in the inner shells occur and increase with increasing κ^* and N [Figs. 9(c) and 10(b)]. For large particle numbers fitting λ becomes more subjective, depending upon which criteria are imposed, e.g., best outermost peak height or inner shell heights. Similarly, increasing the renormalized coupling constant beyond a certain value is only trading agreement from inner to outer shells.

It is curious that the AHNC procedure works so well for pair correlations, both Coulomb and Yukawa, and for the Coulomb trap density profile, but fails for the Yukawa density profile at large κ^* and N. One possible explanation
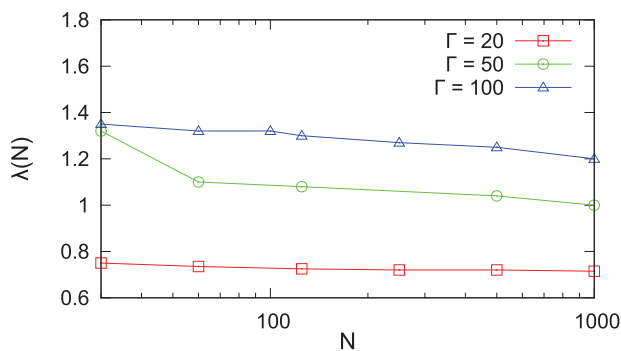

FIG. 8. (Color online) Dependence of the AHNC parameter λ on N for the Coulomb case. The height of the outermost peak is used to obtain λ. The renormalized coupling parameter is given by $\Gamma' = [1 + \lambda(\Gamma)]\Gamma$.
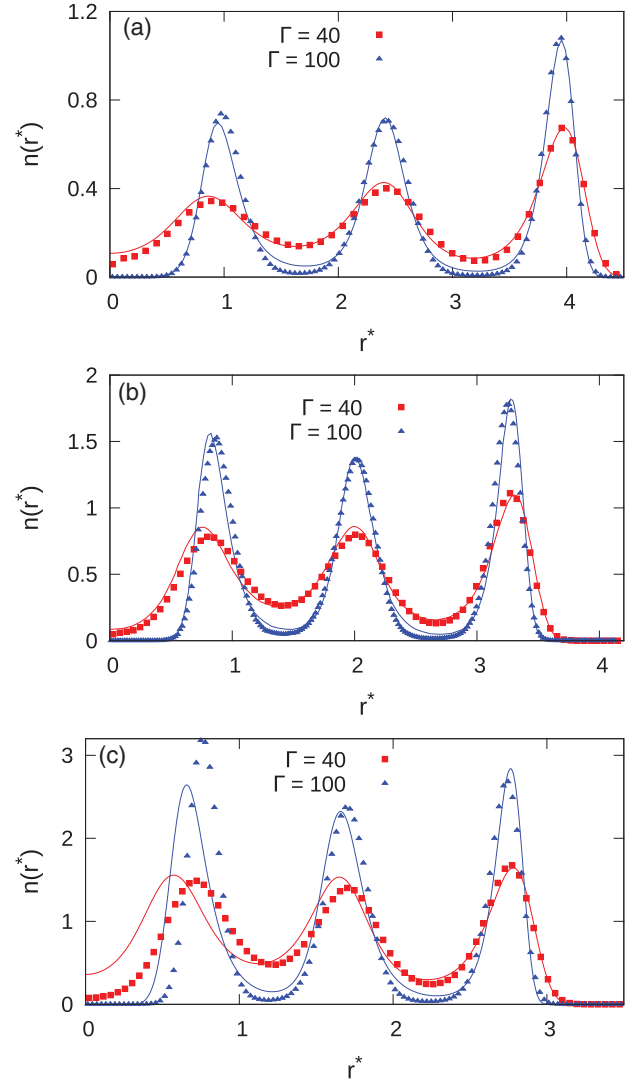

FIG. 9. (Color online) Density profile for $N = 100$ particles: Comparison of AHNC results (lines) and MC data (symbols) for (a) Coulomb interaction, and Yukawa interaction with (b) $\kappa^* = 0.5$ and (c) $\kappa^* = 1$. The renormalized Γ' values used are shown in Fig. 7.

is the following. The density equation of the HNC entails an additional approximation not contained in that for the pair correlations, namely that the pair correlations in the trap can be represented by those of the OCP. This can be justified for Coulomb interactions, but that argument does not extend to Yukawa interactions. At large κ^* this approximation may no longer hold. In addition, the shell structure is enhanced at large κ^*, and the number of shells increases with N. Hence there are increased demands on the AHNC to represent more complex structure.

There is a qualitative difference between the Coulomb and Yukawa cases at large N. In the former case, the harmonic trap is exactly equal to the effect of a uniform neutralizing background, and the system approaches the Coulomb OCP for large N except at the boundaries. However, for the Yukawa case the relationship of the trap to the neutralizing background
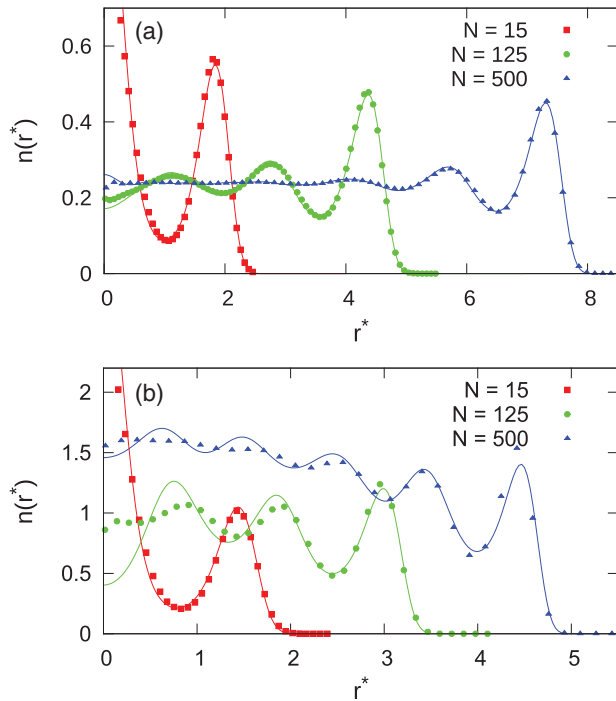
FIG. 10. (Color online) Density profile for a fixed coupling constant $\Gamma = 20$ and various particle numbers: comparison of AHNC results (lines) and MC data (symbols) for (a) a Coulomb and (b) a Yukawa system with $\kappa^* = 1$. Disagreement in the inner part is increasing with particle number for the Yukawa system.

no longer holds. Totsuji *et al.* have derived the corresponding confinement potential for a Yukawa system [26,27].

V. DISCUSSION

A theoretical description is developed for the shell structure of spherically confined Yukawa plasmas. While the precise shell occupations are well known from computer simulations, both for trapped Coulomb, e.g., [12,13], and Yukawa plasmas, e.g., [11], it is desirable to have an analytical theory that correctly reproduces these results and provides physical insight into the correlation properties. Classical density functional theory is the proper starting point for this. In particular, it has been shown that the HNC approximation is able to provide the density profile (the formation, shape, location, and population of shells) accurately for weak to moderate coupling ($\Gamma < 10$). However, HNC fails to reproduce the correct width of the shells.

A simple representation of the bridge functions B (corrections to HNC) called the adjusted HNC (AHNC) is able to provide quantitative agreement in the case of Coulomb interactions for $\Gamma \leqslant 100$ and $N \leqslant 500$, indicating that a simple renormalization of the HNC is sufficient to capture the structural effects of confinement. A similar adjusted HNC provides substantial improvement for the isotropically trapped Yukawa system as well. While it correctly reproduces the shape of the outermost shell(s) that host the majority of particles, it is less accurate for the inner shells, in particular with increasing screening parameter and particle number.

ACKNOWLEDGMENTS

[1] A. V. Filinov, M. Bonitz, and Y. E. Lozovik, Phys. Rev. Lett. **86**, 3851 (2001).

[2] D. J. Wineland, J. C. Bergquist, W. M. Itano, J. J. Bollinger, and C. H. Manney, Phys. Rev. Lett. **59**, 2935 (1987).

[3] M. Drewsen, C. Brodersen, L. Hornekær, J. S. Hangst, and J. P. Schiffer, Phys. Rev. Lett. **81**, 2878 (1998).

[4] G. E. Morfill and A. V. Ivlev, Rev. Mod. Phys. **81**, 1353 (2009).

[5] M. Bonitz, C. Henning, and D. Block, Rep. Prog. Phys. **73**, 066501 (2010).

[6] S. L. Gilbert, J. J. Bollinger, and D. J. Wineland, Phys. Rev. Lett. **60**, 2022 (1988).

[7] O. Arp, D. Block, A. Piel, and A. Melzer, Phys. Rev. Lett. **93**, 165004 (2004).

[8] S. W. S. Apolinario and F. M. Peeters, Phys. Rev. E **83**, 041136 (2011).

[9] J. Cioslowski and E. Grzebielucha, J. Chem. Phys. **134**, 124305 (2011).

[10] H. Kählert and M. Bonitz, Phys. Rev. E **83**, 056401 (2011).

[11] M. Bonitz, D. Block, O. Arp, V. Golubnychiy, H. Baumgartner, P. Ludwig, A. Piel, and A. Filinov, Phys. Rev. Lett. **96**, 075001 (2006).

[12] R. Rafac, J. P. Schiffer, J. S. Hangst, D. H. E. Dubin, and D. J. Wales, Proc. Natl. Acad. Sci. USA **88**, 483 (1991).

[13] P. Ludwig, S. Kosse, and M. Bonitz, Phys. Rev. E **71**, 046403 (2005).

[14] J. Wrighton, J. W. Dufty, C. Henning, and M. Bonitz, J. Phys. A **42**, 547052 (2009).

[15] J. Wrighton, J. W. Dufty, H. Kählert, and M. Bonitz, Phys. Rev. E **80**, 066405 (2009).

[16] J. Wrighton, J. W. Dufty, H. Kählert, and M. Bonitz, Contrib. Plasma Phys. **50**, 26 (2010).

[17] K.-C. Ng, J. Chem. Phys. **61**, 2680 (1974).

[18] J.-P. Hansen and I. MacDonald, *Theory of Simple Liquids* (Academic Press, San Diego, CA, 1990).

[19] C. Henning *et al.*, Phys. Rev. E **74**, 056403 (2006); **76**, 036404 (2007).

[20] V. Golubnychiy, H. Baumgartner, M. Bonitz, A. Filinov, and H. Fehske, J. Phys. A: Math. Gen. **39**, 4527 (2006).

[21] H. Baumgartner, H. Kählert, V. Golubnychiy, C. Henning, S. Käding, A. Melzer, and M. Bonitz, Contrib. Plasma Phys. **47**, 281 (2007).

[22] Y. Rosenfeld and N. Ashcroft, Phys. Rev. A **20**, 1208 (1979).

[23] P. Poll, N. Ashcroft, and H. DeWitt, Phys. Rev. A **37**, 1672 (1988).

[24] W. Daughton, M. Murillo, and L. Thode, Phys. Rev. E **61**, 2129 (2000).

[25] T. Ott, M. Stanley, and M. Bonitz, Phys. Plasmas **18**, 063701 (2011).

[26] H. Totsuji, C. Totsuji, T. Ogawa, and K. Tsuruta, Phys. Rev. E **71**, 045401 (2005).

[27] H. Totsuji, T. Ogawa, C. Totsuji, and K. Tsuruta, Phys. Rev. E **72**, 036406 (2005).